Energy-Minimized Structures and Packing States of a Homologous Series of Mixed-Chain Phosphatidylcholines: A Molecular Mechanics Study on the Diglyceride Moieties

Shusen Li, Zhao-qing Wang, Hai-nan Lin, and C. Huang
Department of Biochemistry, Health Sciences Center, University of Virginia, Charlottesville, Virginia, USA

ABSTRACT Phosphatidylcholines or C(*X*):C(*Y*)PC, quantitatively the most abundant lipids in animal cell membranes, are structurally composed of two parts: a headgroup and a diglyceride. The diglyceride moiety consists of the glycerol backbone and two acyl chains. It is the wide diversity of the acyl chains, or the large variations in *X* and *Y* in C(*X*):C(*Y*)PC, that makes the family of phosphatidylcholines an extremely complex mixture of different molecular species. Since most of the physical properties of phospholipids with the same headgroup depend strongly on the structures of the lipid acyl chains, the energy-minimized structure and steric energy of each diglyceride moiety of a series of 14 molecular species of phosphatidylcholines with molecular weights identical to that of dimyristoylphosphatidylcholine without the headgroup are determined in this communication by molecular mechanics (MM) calculations. Results of two types of trans-bilayer dimer for each of the 14 molecular species of phosphatidylcholines are also presented; specifically, the dimeric structures are constructed initially based on the partially interdigitated and mixed interdigitated packing motifs followed subsequently by the energy-minimized refinement with MM calculations. Finally, tetramers with various structures to model the lateral lipid-lipid interactions in a lipid bilayer are considered. Results of laborious MM calculations show that saturated diacyl C(*X*):C(*Y*)PC with $\Delta C/CL$ values greater than 0.41 prefer topologically to assemble into tetramers of the mixed interdigitated motif, and those with $\Delta C/CL$ values less than 0.41 prefer to assemble into tetramers with a repertoire of the partially interdigitated motif. Here, $\Delta C/CL$, a lipid asymmetry parameter, is defined as the normalized acyl chain length difference between the *sn*-1 and *sn*-2 acyl chains for a C(*X*):C(*Y*)PC molecule; an increase in $\Delta C/CL$ value is an indication of increasing asymmetry between the two lipid acyl chains. These computational results are in complete accord with the calorimetric data presented previously from this laboratory (H-n. Lin, Z-q. Wang, and C. Huang. 1991. *Biochim. Biophys. Acta.* 1067:17–28).

INTRODUCTION

Over the past 3 years, our laboratory has semisynthesized more than 100 molecular species of saturated diacyl mixed-chain phosphatidylcholines or C(*X*):C(*Y*)PC, and the thermotropic phase behavior of the aqueous lipid dispersions prepared from these C(*X*):C(*Y*)PC has been investigated systematically by high-resolution differential scanning calorimetry or DSC (Bultmann et al., 1991; Huang et al., 1993a; Lin et al., 1990, 1991; Wang et al., 1990). Based on the extensive DSC results and the related structural information, some of the structure-property relationships of the self-assembled fully hydrated phospholipids are delineated. We can take three experimental findings as examples to illustrate the contributions of the recent DSC studies to our better understanding of the lipid bilayer system in general:

1. It is possible to correlate quantitatively the main phase transition temperature, T_m, of aqueous lipid dispersions prepared from a specific phospholipid species with the structural characteristics of that lipid in the gel-state bilayer. Consequently, one can successfully predict the T_m values with high precision for fully hydrated bilayers prepared individually from more than 250 molecular species of C(*X*):C(*Y*)PC (Huang et al., 1993a,b).

2. The predictable mixing behavior of two species of phospholipids serves to illustrate the critical role played by the acyl chains of phospholipids in the lipid-lipid interaction. For instance, if identical-chain phosphatidylcholine molecules are mixed with mixed-chain phosphatidylcholines with the same molecular weight (MW), and the two acyl chains of the mixed-chain phosphatidylcholine are so highly asymmetric that one chain is twice the length of the other, these two species of phosphatidylcholines will mix with each other in the liquid-crystalline state but they will be phase-separated in the gel state (Bultmann et al., 1991; Sisk et al., 1990; Slater et al., 1992). This eutectic phase behavior has important biological implications (Huang, 1990).

3. The effect of the acyl chain asymmetry on the main phase transition behavior of fully hydrated phosphatidylcholines has been extensively studied (Huang, 1990; Lin et al., 1991). Interestingly, the effect is biphasic in nature. For

Received for publication 15 April 1993 and in final form 21 June 1993.

Address reprint requests to Dr. Ching-hsien Huang, Department of Biochemistry, Box 440, Health Sciences Center, University of Virginia, Charlottesville, VA 22908.

Abbreviations used: C(*X*):C(*Y*)PC, saturated 1,2-diacyl-*sn*-glycero-3-phosphocholine with *X* carbons in the *sn*-1 acyl chain and *Y* carbons in the *sn*-2 acyl chain; E_s, the steric energy, obtained with the computer program MM2, corresponding to the energy-minimized structure of the calculated molecule; E_m, the steric energy corresponding to the energy-minimized monomeric structure of a lipid molecule; E_d, the steric energy corresponding to the energy-minimized dimeric structure of lipid molecules; MM, molecular mechanics; MW, molecular weight; T_m, phase transition temperature.

0006-3495/93/10/1415/14 $2.00

identical-chain and slightly asymmetric phosphatidylcholines, the main phase transition temperature, T_m, or transition enthalpy, ΔH, decreases with increasing chain asymmetry. For highly asymmetric lipids, however, the trend is reversed. This biphasic phenomenon is very similar to the well-established effect of alcohol on the phase transition temperature of C(16):C(16)PC or C(18):C(18)PC (Nambi et al., 1988; Ohki et al., 1990; Roth and Chen, 1991; Rowe, 1983, 1992).

Quantitatively, the lipid asymmetry for a phosphatidylcholine molecule in the gel-state bilayer can be represented by a structural parameter, $\Delta C/CL$, called the normalized chain length difference, where ΔC is the apparent chain length difference, in C-C bond lengths, between the two acyl chains and CL is the effective length of the longer of the two acyl chains, also in C-C distance along the chain (Huang, 1990; Mason et al., 1981). When the thermodynamic parameters (T_m, ΔH, and ΔS) associated with the main phase transition, obtained from a series of phosphatidylcholines with the same MW but different acyl chain asymmetry, are plotted against the values of $\Delta C/CL$, a biphasic profile is invariably observed. Specifically, within the range of $\Delta C/CL$ values of 0.09–0.41, the T_m (or ΔH) values appear to fall on a linear curve with the minimum value at $\Delta C/CL$ of ~0.41. Beyond the minimum value, the T_m (or ΔH) values increase with increasing values of $\Delta C/CL$ and the data fall on a bell-shaped curve with the maximum value of T_m at $\Delta C/CL$ of about 0.56.

The biphasic phenomenon has been observed for four series of mixed-chain phosphatidylcholines (Bultmann et al., 1991; Lin et al., 1990, 1991). The data are taken to suggest that mixed-chain phosphatidylcholines with $\Delta C/CL$ values less than 0.41 are packed at $T < T_m$ into the partially interdigitated motif in which the *sn*-1 acyl chain of one phospholipid packs end to end with the *sn*-2 acyl chain of another phospholipid from the opposing bilayer leaflet, and the linear decrease in T_m is due to the progressive decrease in the chain-chain contact interactions as a result of increasing values of $\Delta C/CL$. Beyond the value of $\Delta C/CL$ of about 0.41, the highly asymmetric phosphatidylcholines are packed at $T < T_m$ into the mixed interdigitated motif, in which the long acyl chain spans the whole width of the bilayer's hydrocarbon core and the shorter chains, each from a lipid molecule in the opposing leaflet, meet end to end in the bilayer midplane. This change in molecular packing motif results in a biphasic V-shaped profile of the experimental points in the T_m (or ΔH) versus $\Delta C/CL$ plot (Lin et al., 1991). This simple interpretation of the biphasic phenomenon is reasonable, since highly asymmetric phospholipids with $\Delta C/CL$ values of ~0.55 such as C(18):C(10)PC, C(8):C(18)PC, and C(22):C(12)PC are known from x-ray diffraction studies to pack into the mixed interdigitated bilayer, in excess water, at $T < T_m$ (Hui et al., 1984; Mattai et al., 1987; McIntosh et al., 1984; Shah et al., 1990; Zhu and Caffrey, 1993). An intriguing question still remains: Why do asymmetric phosphatidylcholines change their packing motif from a partially interdigitated to a mixed interdigitated type at a $\Delta C/CL$ value of ~0.41? The answer seems to be related to the difference in the stabilization energy of the various lipids in the two types of packing motif.

Computer-based molecular mechanics (MM) calculations have been extensively applied and successfully used in determining the optimal structure and related steric energy for a wide range of hydrocarbons (Allinger, 1977). The diglyceride moiety of a phospholipid molecule consists primarily of two hydrocarbon chains and the glycerol backbone; hence, the MM-2 program based on a force field developed for hydrocarbon and other-compound computations by Allinger is employed in this investigation to obtain the energy-minimized structure and steric energy for the diglyceride moieties of various lipids and their aggregates. Specifically, attempts are made to calculate the stabilization energy of the diglyceride moieties of various C(X):C(Y)PC as they are aggregated into tetramers and packed in the partially interdigitated and mixed interdigitated modes.

This communication begins with a description of underlying assumptions used in MM calculations in obtaining the energy-minimized structure and steric energy for the diglyceride moiety of C(14):C(14)PC. Based on this energy-minimized structure, various mixed-chain phosphatidylcholines with the same MW as that of C(14):C(14)PC are then considered, and their energy-minimized structures and steric energies are determined by MM calculations. Results for the dimers of C(X):C(Y)PC based on two kinds of trans-bilayer packing motif are then obtained. There follows a development of results for the tetrameric packings and their stabilization energies for various C(X):C(Y)PC with different $\Delta C/CL$ values. These computer-generated results are then compared with the calorimetric data obtained experimentally. Based on the good agreement between the computational and experimental data, we conclude that the energetics underlying the lipid-lipid interaction can be used quantitatively in explaining the biphasic profile observed in the T_m (or ΔH) versus $\Delta C/CL$ plot for mixed-chain phosphatidylcholines. Throughout this communication, C(X):C(Y)PC refer to the diglyceride moieties of mixed-chain phosphatidylcholines.

MATERIALS AND METHODS

Molecular mechanics calculations

The force field employed for the present MM calculations was the MM2 program (Version 85) originally developed by Allinger (1977). In this program, the steric energy, E_s, is given by $E_s = E_{st} + E_b + E_{tor} + E_{dip} + E_{VDW} + E_{sb}$, where E_{st} is the stretching energy of bonds, E_b is the energy associated with the angle bending, E_{tor} is the torsional energy of bonds, E_{dip} is the energy of bond-dipole interactions, E_{VDW} is the energy of van der Waals interactions, and E_{sb} is the energy associated with the coupling between bond stretching and angle bending.

Of the various terms, E_{VDW} plays the most important role in determining the structure and total energy of the diglyceride moiety of lipid molecules. In the Allinger (1977) force field used in this work, the van der Waals interaction has been developed on the basis of the Hill form of the Buckingham potential, and the expression is virtually identical to a Lennard-Jones

or 6–12 potential as follows:

$$E_{VDW} = \sum_{i \neq j} \epsilon_{ij} (2.9 \times 10^5 \exp(-12.5\rho_{ij}) - 2.25\ \rho_{ij}^{-6}) \qquad \text{for } \rho_{ij} \geq 0.302$$

or

$$E_{VDW} = 336.176 \sum_{i \neq j} \epsilon_{ij} \rho_{ij}^{-2} \qquad \text{for } \rho_{ij} \leq 0.302.$$

Where $\rho_{ij} = R_{ij}/\gamma_{ij}^*$, R_{ij} is the distance between nonbonded atoms i and j, and $\gamma_{ij}^* = \gamma_i^* + \gamma_j^*$; γ_i^* and γ_j^* are the van der Waals radii of nonbonded atoms i and j, respectively; $\epsilon_{ij} = \sqrt{\epsilon_i \epsilon_j}$; and ϵ_i is a hardness parameter that determines the depth of the attractive well for atom i. In the MM2 program, van der Waals interactions include atoms with 1–4 vicinal and normal 1–5 and greater nonbonded relationships. Based on the E_{vdw} equation used in MM2, the van der Waals interaction for a nonbonded $C(sp^3)$-$C(sp^3)$ pair is repulsive if the nonbonded carbon-carbon distance is less than 3.34 Å and attractive if it is in the range of 3.34–6.22 Å. For a nonbonded C-H pair, the van der Waals interaction is repulsive, if the nonbonded C-H distance is less than 2.94 Å, and attractive if it is within the range of 2.94–5.46 Å. For a nonbonded H-H pair, the repulsive distance is less than 2.64 Å. Therefore, when two methylene carbons are within the spatial distance of 3.80–4.10 Å, the nonbonded C-C contact interaction is clearly attractive; however, the methylene H-H interaction may be repulsive. By taking the energy-minimized structure of C(14):C(14)PC as an example, C_4 of the *sn*-1 acyl chain is in close proximity to C_7 of the *sn*-2 acyl chain by 4.09 Å, and the energy of the van der Waals interaction, E_{VDW}, is −0.0453 kcal/mol. A hydrogen atom of C_4 of the *sn*-1 acyl chain, on the other hand, is spatially separated from a hydrogen atom of C_7 of the *sn*-2 acyl chain by 2.46 Å, and the corresponding value of E_{VDW} of 0.0231 kcal/mol is positive, indicating a repulsive force. In general, van der Waals interactions are one of the main energetic terms that determine the stability of lipid molecules in aggregated form.

For monomeric lipids such as C(14):C(14)PC, the initial trial set of atomic coordinates has been estimated from the ball-and-stick model, and the assumptions used in building the model are presented later in Results. These coordinates are entered into the computer via the MM2 program. A process of refinement ensues in which by a fitting procedure the various torsion angles of the lipid molecule are systematically adjusted to minimize the overall steric energy. What comes out of the energy minimization calculation is a new set of atomic coordinates, corresponding to a minimum point on the energy surface. Since we are interested primarily in a homologous series of phospholipids with the same headgroup and with the same MW, we can simplify greatly our laborious MM calculations by considering only the diglyceride moiety of the lipid molecule. In this paper, various phospholipids without the headgroups are thus used exclusively for our MM calculations. Consequently, the headgroup-headgroup interaction and the headgroup interaction with diglyceride are not considered in our MM calculations.

For dimers, MM calculations are carried out according to two types of packing motif, i.e., the partially interdigitated and the mixed interdigitated mode. Since these packing motifs specify the geometric arrangements of two lipid molecules each derived from the opposing leaflet of the crystalline bilayer, these dimers are referred as the trans-bilayer dimers. The structures of these trans-bilayer dimers are presented later in Results. The important point is that each type of the initial structure of C(*X*):C(*Y*)PC trans-bilayer dimer is constructed based on the energy-minimized structure of the monomeric species of C(*X*):C(*Y*)PC; the initial structure of the trans-bilayer dimer is subsequently energy-minimized with the MM2 program. Likewise, the tetramer is initially built from two of the energy-minimized structures of the trans-bilayer dimer on the basis of a defined arrangement of nearest neighbors, and the final structure of the tetramer is obtained after subjecting the initial structure to an energy-minimized refinement with the MM2 program. The nomenclatures of E_s for monomeric and dimeric lipids used throughout this communication are E_m and E_d, respectively.

RESULTS AND DISCUSSION

The geometry and steric energy of C(14):C(14)PC obtained from MM calculations

Two x-ray crystallographic structures of C(14):C(14)PC were first described by Pearson and Pascher (1979). These crystal structures, called A and B, are different primarily in the orientation of the polar headgroup with respect to the hydrophobic part. The observed orientational differences between x-ray crystal structures A and B can be attributed to the rotation of the polar headgroup about the glycerol C(2)-C(3) bond (Pearson and Pascher, 1979). The hydrophobic or diglyceride moieties of the two crystallographic structures, however, are roughly similar. Specifically, the diglyceride moieties of molecules A and B exhibit a common h-shaped geometry in which the glycerol carbons, the primary ester oxygens, and all carbons in the *sn*-1 acyl chains are arranged in a virtually straight line, and the *sn*-2 acyl chain is bent at the C_2 position. The torsion angles of the various components of the diglyceride moieties of the x-ray crystal structures A and B are presented in Table 1. The convention for naming the various torsion angles is shown in Fig. 1 *A*.

The minimum energy structure of the diglyceride part of C(14):C(14)PC can be determined from MM calculations using the MM2 program (Allinger, 1977). First, a set of crude torsion angles that approximate the h geometry of C(14):C(14)PC as determined by x-ray crystallography (Pascher et al., 1992) is created from the ball-and-stick molecular model. The crude initial estimations are based on the following four assumptions:

1. The hydrocarbon chain in crystals is basically a zigzag plane of a conformationally regular array of methylene units. The C-C bonds in the *sn*-1 acyl chain and the C-C bonds beyond the C_2 atom in the *sn*-2 acyl chain are thus all *trans*.

2. The bond that links the glycerol oxygen and the carbonyl carbon is the O-C_1 ester bond, where C_1 is the first carbon atom of the fatty acyl chain (Fig. 1 *A*). This ester bond has a partial double-bond character owing to the resonance

TABLE 1 The torsion angles of the various components of the diglyceride moieties of the crystal structures A and B and the energy-minimized structure (C) of C(14):C(14)PC*

Structure	E_s‡	θ_1	θ_2	θ_3	θ_4	β_1	β_2	β_3	β_4	β_5	γ_1	γ_2	γ_3
A	(23.60)§	58	177	−178	63	82	172	−81	45	171	−177	168	−173
B	(19.83)§	168	−80	166	51	120	179	−134	67	180	102	176	180
C	19.53	178	−63	180	61	104	176	−62	−56	178	176	179	173

* The torsional angles for crystal structures A and B are taken from Pascher et al. (1992).

‡ Energy unit: kcal/mol.

§ The steric energy given in parentheses is obtained from the energy-minimized structure of crystal structure A or B as shown in Fig. 3 *A'* or *B'*.

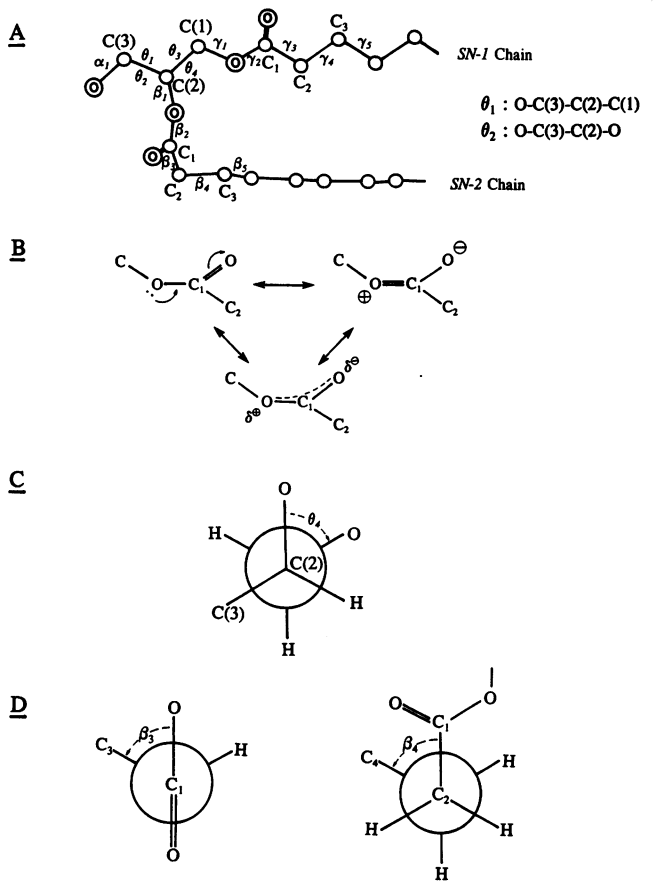

FIGURE 1 The four basic assumptions used in MM calculations in obtaining the energy-minimized structure and steric energy for C(14):C(14)-PC. (*A*) The C-C bonds in the *sn*-1 acyl chain and the C-C bonds beyond the C_2 atom in the *sn*-2 acyl chain are all-*trans*. The convention for naming the various torsion angles (α_n, β_n, γ_n, θ_n) is also indicated. In addition, C(*n*) and C_n are used to denote the various carbon atoms in the glycerol backbone and acyl chains, respectively. (*B*) The ester bond has a substantial fraction of double-bond character due to the resonance hybrid of three forms as shown. (*C*) A torsional angle of 60° is assumed for the O-C(1)-C(2)-O bond (θ_4). (*D*) Two successive *gauche* (−) bonds are assumed to take place in the initial segment of the *sn*-2 acyl chain, resulting in a 90° sharp bend at the C_2 atom.

hybrid effect (Huang, 1977) (Fig. 1 *B*); hence, the primary and secondary ester bonds, which link the *sn*-1 and *sn*-2 acyl chains, respectively, to the glycerol backbone, have *trans* configurations. The energetically preferred *trans* configuration is to render the five atoms in the ester group, C(1 or 2)-O-C_1(=O)-C_2, coplanar at physiological temperatures. Here, C(1) and C(2) denote the carbon atoms 1 and 2 of the glycerol backbone (Fig. 1 *A*), respectively, and C_1 and C_2 are the first and second carbon atoms of the fatty acyl chain, respectively (Fig. 1 *B*).

3. The primary and secondary ester planes are virtually perpendicular to each other. This is a consequence of a unique torsion angle (θ_4) of 60° for the O-C(1)-C(2)-O bond (Fig. 1 *C*). The C(1)-C(2) bond connects contiguously the two ester planes in the lipid molecule.

4. The *sn*-2 acyl chain is bent 90° at the C_2 position (Fig. 1 *A*). This sharp bend is assumed to result from two successive *gauche* (−) configurations in the C_1-C_2 bond (β_3 = −60) and the C_2-C_3 bond (β_4 = −60), as shown in Fig. 1 *D*. Based on the above four basic assumptions, the estimated torsion angles for C(14):C(14)PC in the crystalline state are $\beta_1 = 120°$, $\beta_2 = 180°$, $\beta_3 = -60°$, $\beta_4 = -60°$, $\beta_5 = \cdots \beta_{15} = 180°$, $\gamma_1 = 180°$, $\gamma_2 = 180°$, $\gamma_3 = \cdots \gamma_{15} = 180°$, $\theta_3 = 180°$, and $\theta_4 = 60°$. Using these values, the MM2 program enables the potential energy of the diglyceride part of C(14):C(14)PC to be minimized automatically on the potential energy hypersurface by systematic optimizations of the various torsion angles. The outputs of the computer calculation yield the values of all the torsion angles for the minimum energy structure of the diglyceride part of C(14):C(14)PC, shown in Table 1 under Structure C, and its steric energy (E_s = 19.53 kcal/mol).

As shown in Table 1 under Structure C, the refined values of the various torsion angles for the individual component of the glycerol backbone and acyl chains of C(14):C(14)PC obtained from MM calculations are similar, but not identical, to the corresponding initial values estimated from the ball-and-stick molecular model. Based on these refined values, computer graphics of the diglyceride part of the C(14):C-(14)PC molecule can be generated, and some computer-generated drawings are presented in Fig. 2.

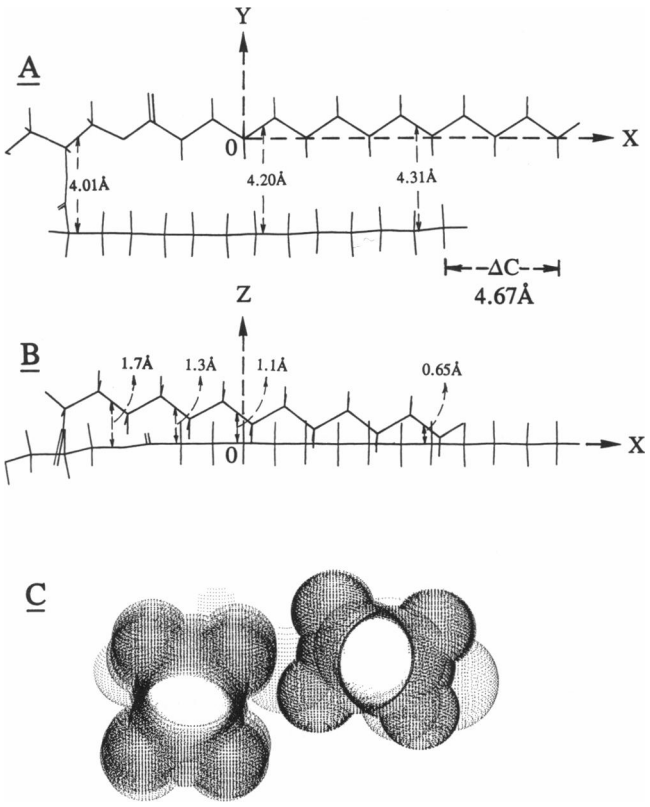

FIGURE 2 The energy-minimized conformation of the diglyceride moiety of C(14):C(14)PC generated by computer graphics. (*A*) The two acyl chains are viewed on the *x*-*y* plane. (*B*) The same structure is viewed on the *x*-*z* plane. (*C*) A projected view of the two acyl chains including their van der Waals radii is shown on the *y*-*z* plane.

Fig. 2 *A* shows that in the energy-minimized structure the fully extended *sn*-1 acyl chain and the *sn*-2 acyl chain beyond C_2 are nearly parallel. In order to specify the orientations of the zigzag planes of the two parallel acyl chains, we assign all the even-numbered carbon atoms in the *sn*-1 acyl chain to lie on a single line defined as the *x*-axis, with the origin of the Cartesian coordinate fixed at C_4. The positive direction of the *x*-axis runs from C_4 to C_{14} along the *sn*-1 acyl chain. We further assign the positive direction of the *y*-axis to run from C_4 to the midpoint of an imaginary line connecting C_3 and C_5, as indicated in Fig. 2 *A*. With these definitions, the zigzag plane of the *sn*-2 acyl chain can be described to lie perpendicularly in front of the zigzag plane of the *sn*-1 acyl chain, and the two zigzag planes are, in the *x*-*y* plane, separated nonuniformly from each other along the *y*-axis (Fig. 2 *A*). The separation distances between some of the carbon atoms in the *sn*-1 acyl chain and the zigzag plane of the *sn*-2 acyl chain, along the *y*-axis, are indicated in Fig. 2 *A*. On the *x*-*z* plane, the separation distances between the carbon atoms of the *sn*-2 acyl chain and the zigzag plane of the *sn*-1 acyl chain are smaller along the *z*-axis, as indicated in Fig. 2 *B*. Furthermore, the chain terminal methyl groups of the two acyl chains are separated from each other along the *x*-axis by 4.67 Å.

A projected view of the two acyl chains down the *x*-axis is shown in Fig. 2 *C*. Since two hydrogen atoms per each carbon atom are directed away from the surface of the long-chain axis, and since odd and even carbons lie on two different lines along the chain, all hydrogen atoms thus form four regular ridges separated by shallow grooves on the surface of each of the acyl chains. It is evident from Fig. 2 *C* that at the interface between the two acyl chains a ridge of one acyl chain fits into a groove of the other and vice versa. This packing geometry is most likely to maximize the van der Waals contact interactions between the two acyl chains within a lipid molecule.

For comparison, the computer graphics of C(14):C(14)PC representing the x-ray crystal structures A and B and the energy-minimized structure are illustrated in Fig. 3 (*A, B,* and *C,* respectively). In these graphics, the *sn*-2 acyl chains of all three structures are topologically aligned in the same orientation. Obviously, the minimum energy structure, shown in Fig. 3 *C*, is roughly equivalent to the x-ray crystal structure B, shown in Fig. 3 *B*, in which the two zigzag planes are nearly perpendicular to each other. However, the *sn*-1 acyl chain bends upward toward the $+y$ direction in the x-ray crystal structure B. Fig. 3 *A* shows the diglyceride conformation of the x-ray crystal structure A for C(14):C(14)PC. In this structure, the relative positions of the two fully extended acyl chains are observed to show an even greater deviation from the paradigm of the parallel packing. In fact, one chain runs over the other at a segment between the C_4-C_6 bond of the *sn*-1 acyl chain and the C_8-C_{10} bond of the *sn*-2 acyl chain. At this crossover region, substantial repulsive interactions between the two acyl chains exist.

After energy minimization, the crystal structures A and B are modified somewhat; the graphics displays of the modified structures A′ and B′ are shown in Fig. 3 (*A′* and *B′*, respectively). From these figures, it is evident that structures A and A′ are remarkably similar. Moreover, the modified structure B′ and the energy-minimized structure C also appear to be similar. A closer examination, however, indicates that the *sn*-2 acyl chain in B′ is not quite as straight as that in C. This curvilinear *sn*-2 acyl chain would reduce its ability to undergo full-length, closest van der Waals contact interactions with adjacent straight chains. Furthermore, if the modified structure B′ is viewed down the *y*-axis, the *sn*-1 and *sn*-2 acyl chains can be seen to cross over each other, again indicating that the two adjacent intramolecular acyl chains are nonparallel. MM calculations yield the steric energies for structures A′ and B′ (Table 1); these values are, respectively, 4.07 and 0.30 kcal/mol greater than the steric energy of the minimum energy structure C. The unfavorable energies of A′ and B′ together with their unparallel acyl chain conformations make them difficult to consider as possible monomeric structures for C(14):C(14)PC in the lipid bilayer in the crystalline state. This difficulty arises from the fact that x-ray diffraction studies on phosphatidylcholines in the crystalline bilayer show that the hydrocarbon chains are highly ordered with strong lateral chain-chain interactions (Ruocco and Shipley, 1982). On the other hand, the minimum energy structure of C(14):C(14)PC with two nearly parallel acyl chains, shown in Fig. 3 *C*, can be reasonably considered as the preferred conformation of C(14):C(14)PC molecule in the lipid bilayer at temperatures below the subtransition temperature. Not only is this structure the most stable one in terms of intramolecular potential energy, but it also can promote the most favorable van der Waals interactions with neighboring chains in the bilayer at low temperatures due to

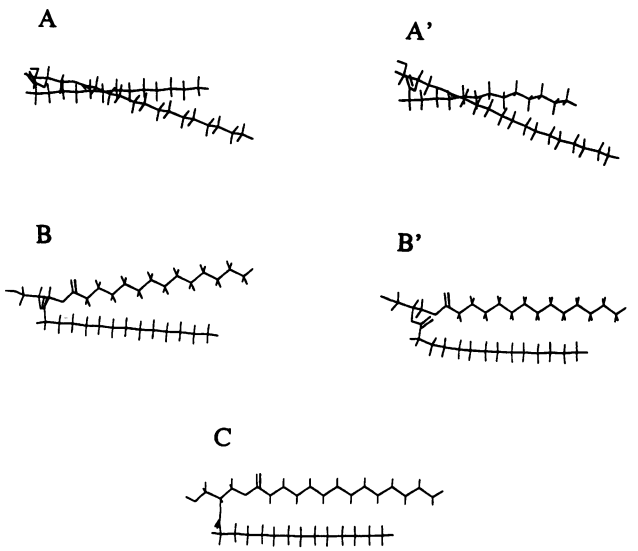

FIGURE 3 The computer graphics of the diglyceride moiety of C(14):C(14)PC. (*A*) The x-ray crystal structure A; (*A′*) the energy-minimized structure of A. (*B*) The x-ray crystal structure B; (*B′*) the energy-minimized structure of B. (*C*) The energy-minimized structure based on the four assumptions presented in Fig. 1 and obtained by MM calculations with the MM2 program.

its virtually linear and parallel acyl chains. The lipid structure shown in Fig. 3 *C* is thus taken as the basic equilibrium molecular structure of C(14):C(14)PC in the crystalline phase of the bilayer for our subsequent studies and calculations. Of course, the equilibrium molecular structure refers, throughout this paper, to the diglyceride part of the lipid molecule. In other words, the energy-minimized structure of the diglyceride part of the phosphatidylcholine molecule shown in Fig. 3 *C* is taken to represent the equilibrium molecular structure of the lipid molecule without its headgroup. It should be emphasized that the zigzag planes of the two acyl chains in the energy-minimized structure are perpendicular to each other. This structural feature has been detected recently by Lewis and McElhaney (1992) using the FT-infrared spectroscopic technique for the C(14):C(14)PC bilayer in the subgel or crystalline phase. Moreover, the energy-minimized structure with two acyl chains of perpendicular zigzag planes differs from the one proposed by Vanderkooi (1991), wherein the zigzag planes of the two acyl chains are parallel.

The intramolecular potential energies of a series of 14 molecular species of phosphatidylcholines with a constant molecular weight of 678.0

After we have determined the energy-minimized conformation and the steric energy of monomeric C(14):C(14)PC, we turn now to examine the changes in the structure and energy of the diglyceride moiety of monomeric C(14):C(14)PC as the two acyl chains contained in the lipid molecule make progressive and reverse alterations in their chain lengths.

As shown in Figs. 1 and 2, the *sn*-1 acyl chain of C(14):C(14)PC is ester-linked to C(1) of the glycerol backbone. Hence, the length of the zigzag plane extending from the glycerol backbone to the chain terminal methyl end is longer than that of the *sn*-1 acyl chain by an initial segment comprising the C(2)-C(1)-O-C_1 moiety. The *sn*-2 acyl chain, however, is shortened by 1.2 Å due to the 90° bend at C_2. The difference between the extended *sn*-1 acyl chain and the shortened *sn*-2 acyl chain along the long molecular *x*-axis is defined as the effective chain length difference between the two acyl chains denoted as ΔC. For the equilibrium molecular structure of C(14):C(14)PC shown in Fig. 2, the value of ΔC is 4.67 Å or 3.68 C-C bond distance along the chain. If a methylene unit is removed from the *sn*-2 acyl chain in C(14):C(14)PC in the crystalline state and then added back to the *sn*-1 acyl chain, the resulting molecule of C(15):C(13)PC will have the same MW as that of C(14):C(14)PC. This process, however, leads to an increase in the lipid asymmetry. The lipid asymmetry can be expressed quantitatively by the structural parameter of ΔC. For mixed-chain C(15):C(13)PC, the value of ΔC can be obtained from the energy-minimized structure, and it is 7.19 Å or 5.66 C-C bond distance along the chain.

If we express the effective chain length difference between the two acyl chains in C(14):C(14)PC as the reference state (ΔC_{ref}), then the effective chain length difference between the two acyl chains in a C(*X*):C(*Y*)PC molecule in the crystalline bilayer can be approximated, in terms of C-C bond lengths along the chain, by the equation $\Delta C = (X - 1) - (Y - 1 - \Delta C_{ref}) = X - Y + \Delta C_{ref}$, where *X* and *Y* are the number of carbons in the *sn*-1 and *sn*-2 acyl chains, respectively. For crystalline C(15):C(13)PC, the value of ΔC can be estimated as follows: $\Delta C = 15 - 13 + 3.68 = 5.68$ C-C bond lengths along the chain. Since a single C-C bond length along the chain is 1.27 Å, the value of ΔC can be expressed as 7.21 Å, which is in excellent agreement with the value of 7.19 Å determined by MM calculations for C(15):C(13)PC in the crystalline bilayer.

As the absolute ΔC value increases stepwise, one can expect that the intramolecular chain-chain contact interaction will decrease successively, resulting in a progressive increase in E_m. This expectation is indeed borne out by MM calculations. Table 2 shows the results of MM calculations obtained with a series of mixed-chain phosphatidylcholines in which the number of carbon atoms in the *sn*-1 acyl chain increases stepwise from 7 to 20 and the number of carbons in the *sn*-2 acyl chain decreases simultaneously from 21 to 8. All these mixed-chain lipids have a common MW of 678.0, but their ΔC values vary from −13.13 Å for C(7):C(21)PC to 19.92 Å for C(20):C(8)PC. In this table, the values of E_m,

TABLE 2 The calculated energies and ΔC values for a homologous series of mixed-chain phosphatidylcholines or C(*X*):C(*Y*)PC*

Lipid	E_m	$E^{1.4}{}_{VDW}$	$E^{other}{}_{VDW}$	ΔE_m	$\Delta E^{1.4}{}_{VDW}$	$\Delta E^{other}{}_{VDW}$	ΔC (Å)
C(20):C(8)PC	24.42	26.33	−11.69	5.87	−0.04	5.87	19.92
C(19):C(9)PC	23.68	26.37	−12.43	5.13	0.0	5.13	17.33
C(18):PC(10)PC	22.79	26.36	−13.23	4.24	−0.01	4.33	14.84
C(17):C(11)PC	22.03	26.40	−14.08	3.48	0.02	3.48	12.26
C(16):C(12)PC	21.14	26.38	−14.97	2.59	0.01	2.59	9.76
C(15):C(13)PC	20.38	26.41	−15.75	1.79	0.04	1.81	7.19
C(14):C(14)PC	19.52	26.41	−16.59	0.97	0.04	0.97	4.67
C(13):C(15)PC	18.93	26.42	−17.20	0.38	0.05	0.36	2.11
C(12):C(16)PC	18.55	26.37	−17.56	0.0	0.0	0.0	−0.39
C(11):C(17)PC	19.13	26.39	−17.02	0.58	0.02	0.54	−2.96
C(10):C(18)PC	19.59	26.39	−16.53	1.04	0.02	0.99	−5.45
C(9):C(19)PC	20.74	26.34	−15.40	2.19	−0.03	2.16	−8.04
C(8):C(20)PC	21.24	26.37	−14.89	2.69	0.0	2.67	−10.53
C(7):C(21)PC	22.40	26.36	−13.73	3.85	−0.01	3.83	−13.13

* All of the energy terms (*E*) have the unit of kcal/mol.

$E^{1,4}_{VDW}$, and E^{other}_{VDW} are listed. The term $E^{1,4}_{VDW}$ describes the total van der Waals interactions arising from atoms with a 1–4 vicinal relationship; hence, it represents primarily the intrachain's nonbonded interactions. The values of $E^{1,4}_{VDW}$ for all the lipids shown in Table 2 are virtually identical; this can be attributed to the fact that all these lipids have the same total number of methylene units in their acyl chains. The term E^{other}_{VDW} describes the total van der Waals interactions for nonbonded pairs of atoms, excluding all 1–4 pairs; hence, it represents primarily the interchain contact interactions. It is interesting to note that the values of E_m and E^{other}_{VDW}, shown in Table 2, are a linear function of the absolute value of ΔC for the various lipids under study. The smallest values of E_m and E^{other}_{VDW} are observed for C(12):C(16)PC, which has the smallest absolute value of ΔC. If we subtract from each E_m value shown in Table 2 the E_m value of C(12):C(16)PC, the difference, ΔE_m, can then be used to assess the energy contribution from the difference in the lipid acyl chain alone. The values of ΔE_m for various lipids are given in Table 2, column 5. In addition, the difference between the E^{other}_{VDW} value and the minimum value of E^{other}_{VDW} for C(12):C(16)PC, ΔE^{other}_{VDW}, for each asymmetric lipid is presented in Table 2, column 7. It is evident that the values of ΔE_m and ΔE^{other}_{VDW} for a given mixed-chain phosphatidylcholine molecule shown in Table 4 are virtually identical, indicating that the difference in the steric energy between two asymmetric lipid molecules with the same headgroup and MW but different acyl chain lengths can be attributed entirely to their difference in the chain-chain van der Waals interaction.

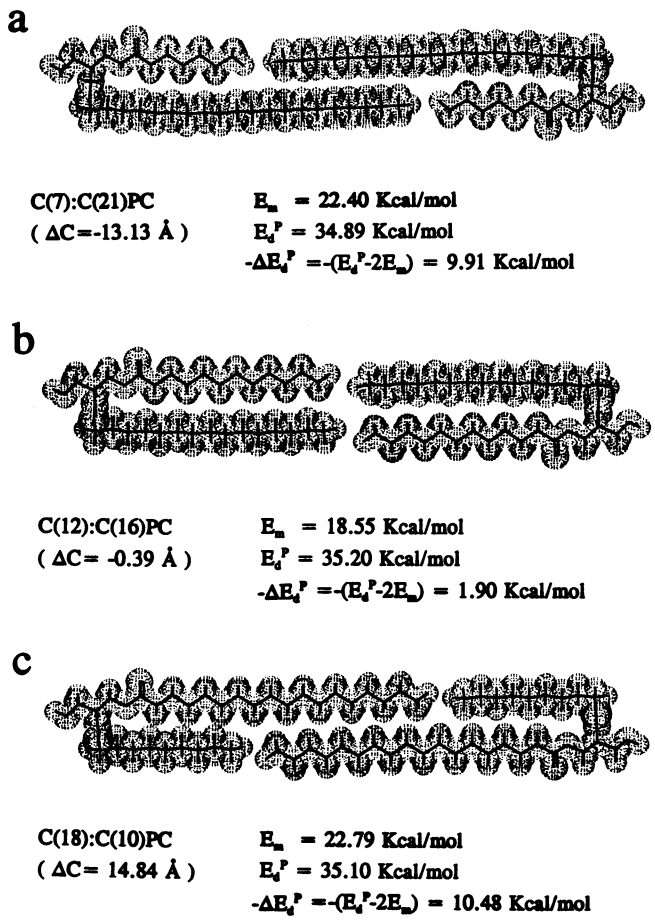

FIGURE 4 The energy-minimized structures of three examples of dimeric C(X):C(Y)PC constructed on the basis of a partially interdigitated packing motif.

Packing preference of C(*X*):C(*Y*)PC in partially interdigitated and mixed interdigitated dimers

Now we have determined the steric energies for 14 molecular species of monomeric C(*X*):C(*Y*)PC with a common MW of 678.0 but different chain asymmetry (ΔC), our next approach is to determine the packing preference of this series of lipids (without the headgroup) as they are aggregated into trans-bilayer dimers. Specifically, two types of packing motif are considered: a partially interdigitated and a mixed interdigitated packing type.

Fig. 4 shows the energy-minimized structures of three examples of dimeric C(*X*):C(*Y*)PC as they are constructed based on the partially interdigitated packing motif. In this packing mode, the short chain of one lipid molecule from one leaflet aligns with the long chain of the second lipid molecule from the opposing leaflet and vice versa; moreover, the spacing between the two opposing terminal methyl carbons along the aligned chain axis is initially taken to be the van der Waals contact distance (~4.10 Å).

In the case of C(7):C(21)PC, the *sn*-2 acyl chain is considerably longer than the *sn*-1 acyl chain, and the ΔC value is −13.13 Å, where the negative sign indicates that the *sn*-1 acyl chain is shorter than the *sn*-2 acyl chains. Fig. 4 *a* shows that in the partially overlapped region, the intermolecular chain-chain contact between two adjacent *sn*-2 acyl chains extends from C_{14} to C_{21} in each chain. Since the two *sn*-2 acyl chains run in the opposite direction, C_{14} of one chain is in closest van der Waals contact by about 3.95 Å with C_{21} of the neighboring chain. Likewise, C_{15}, C_{16}, C_{17}, C_{18}, C_{19}, and C_{20} of one chain are each in close van der Waals contact with C_{20}, C_{19}, C_{18}, C_{17}, C_{16}, and C_{15}, respectively, of the neighboring chain. These multiple intermolecular van der Waals contacts make significant contributions to the stability of C(7):C(21)PC dimer. The overall steric energy of this trans-bilayer dimer, E_d^P, is 34.89 kcal/mol, and the steric energy for the monomer, E_m, is 22.40 kcal/mol (Table 2, column 2). The intermolecular chain-chain interaction energy in the trans-bilayer dimer can thus be calculated to be $\Delta E_d^P = (E_d^P - 2E_m) = -9.91$ kcal/mol.

Fig. 4 *b* shows the energy-minimized structure of a C(12):C(16)PC trans-bilayer dimer packed in the partially interdigitated mode. The two acyl chains within each monomer have nearly identical effective chain lengths ($\Delta C = -0.39$ Å). Consequently, the intramolecular chain-chain interactions dominate over the intermolecular interactions. Furthermore, Fig. 4 *b* also shows that intramolecularly only even carbons in the *sn*-1 acyl chain are in close van der Waals contact with the methylene units of the neighboring *sn*-2 acyl chains. The

total steric energy of the dimeric C(12):C(16)PC packed in the partially interdigitated mode, E_d^P, can be calculated by the MM2 program to be 35.20 kcal/mol. This value is larger than that of dimeric C(7):C(21)PC by about 0.3 kcal/mol, indicating that the C(12):C(16)PC trans-bilayer dimer is slightly more unstable. Based on the limited intermolecular contact surface for the C(12):C(16)PC dimer shown in Fig. 4 *b*, one would also expect that the intermolecular interaction energy within the trans-bilayer dimer is smaller. Indeed, a ΔE_d^P value of −1.90 kcal/mol confirms our expectation. Fig. 4 *c* shows the computer graphics of a C(18):C(10)PC trans-bilayer dimer packed according to the partially interdigitated motif. The intermolecular chain-chain contact interactions are seen to occur primarily between two neighboring *sn*-1 acyl chains. The chain length difference between the *sn*-1 and *sn*-2 acyl chains (ΔC) in C(18):C(10)PC is 14.84 Å; hence, the overlapping region in the partially interdigitated packing motif is quite long, extending from C_9 to C_{18} in each *sn*-1 acyl chain. However, only even carbons in the *sn*-1 acyl chain undergo van der Waals contact interactions with even carbons of the adjacent *sn*-1 acyl chain. Each even carbon in the overlapping region is, in fact, in close juxtaposition to two even carbons of the neighboring chain. For instance, the separation distances between C_{14} of one chain and C_{12} and C_{14} of the adjacent chain are 3.98 and 3.74 Å, respectively. These multiple van der Waals contacts can make a substantial stabilizing contribution to the structure of C(18):C(10)PC trans-bilayer dimer. The steric energy of dimeric C(18):C-(10)PC packed in the partially interdigitated mode has been calculated by the MM2 program to be 35.10 kcal/mol. The intermolecular chain-chain interaction thus makes a negative (stabilizing) energy contribution, $\Delta E_d^P = E_d^P - 2E_m = -10.48$, to the overall energy of the C(18):C(10)PC trans-bilayer dimer.

Fig. 5 gives the energy-minimized structures of the trans-bilayer dimers of C(7):C(21)PC, C(12):C(16)PC, and C(18):C(10)PC as they are obtained from MM calculations on the basis of the mixed interdigitated packing motif. The steric energy (E_d^M) and the intermolecular interaction energy (ΔE_d^M) for trans-bilayer dimers constructed based on 14 different molecular species of lipids are summarized in Table 3. In this mixed interdigitated packing mode, the long acyl chain spans the entire bilayer width while the terminal methyl groups of the short chains, each from a lipid molecule in the opposing leaflet, meet end to end in the bilayer midplane.

In the case of C(7):C(21)PC, the zigzag planes of the two shorter *sn*-1 acyl chains are virtually coplanar, and their long molecular axes are aligned along the same line but in opposite directions (Fig. 5 *a*). All the methylene carbons of the shorter *sn*-1 acyl chains are in closest van der Waals contacts with the methylene units of two neighboring *sn*-2 acyl chains. It should be noted that in the partially interdigitated packing motif, only even carbons in the *sn*-1 acyl chain participate in the chain-chain contact interactions (Fig. 4). Hence, the steric energy of dimeric C(7):C(21)PC can be expected to reduce somewhat when the lipid packing motif is converted from the partially interdigitated to the mixed interdigitated type. Indeed, the steric energy of dimeric C(7):C(21)PC is calculated to change from a value of 34.89 kcal/mol, corresponding to the partially interdigitated packing motif, to a smaller value of 31.40 kcal/mol, corresponding to the mixed interdigitated packing motif (Table 3). Moreover, the intermolecular interaction energy (ΔE_d^M) calculated for dimeric C(7):C-(21)PC also changes from −9.91 kcal/mol to −13.4 kcal/mol as the packing motif of the C(7):C(21)PC trans-bilayer dimer converts from a partially interdigitated to a mixed interdigitated type (Table 3). These data thus indicate that the lateral chain-chain contact interactions in a mixed interdigitated dimer are more extensive; consequently, they make significantly more contributions to the overall stability of a mixed interdigitated C(7):C(21)PC dimer.

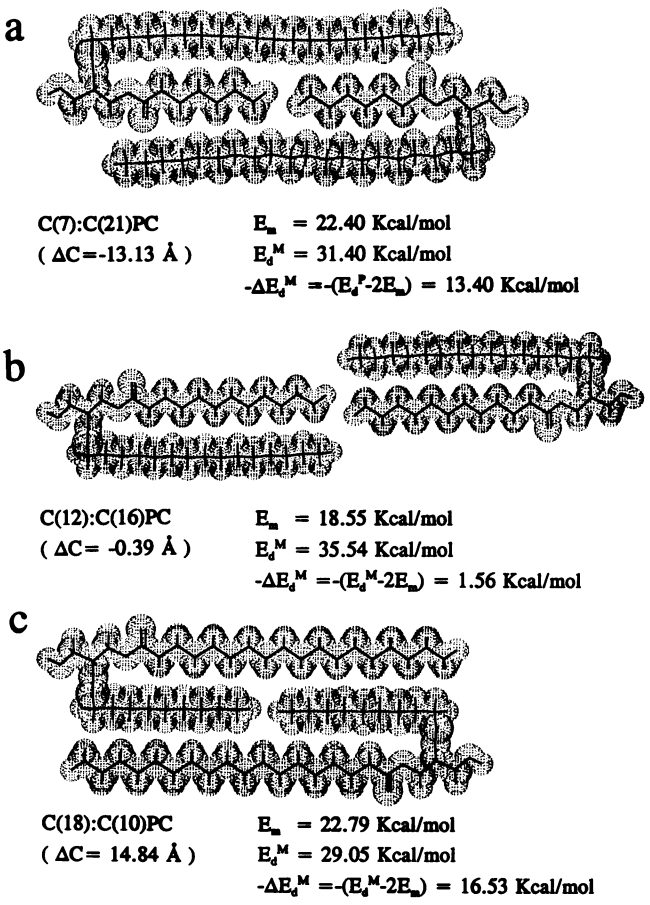

FIGURE 5 Three examples of dimeric C(X):C(Y)PC constructed on the basis of a mixed interdigitated packing motif.

For C(12):C(16)PC, the major intermolecular interaction within a mixed interdigitated dimer is the van der Waals contact interaction between the two opposing terminal methyl groups of the *sn*-1 acyl chains. This rather limited chain-chain contact interaction can be attributed to the small value (−0.39 Å) of ΔC (Fig. 5 *b*). The calculated value of E_d^M for dimeric C(12):C(16)PC in a mixed interdigitated packing mode is 35.54 kcal/mol, which is only 0.34 kcal/mol larger than that calculated for dimeric C(12):C(16)PC packed in the partially interdigitated mode (Fig. 4 *b*). This example thus illustrates the fact that trans-bilayer dimers formed from

TABLE 3 The steric energies for partially interdigitated (E^P_d) and mixed interdigitated (E^M_d) dimers of a homologous series of mixed-chain phosphatidylcholines*

Lipid	E^P_d	E^M_d	$-\Delta E^P_d$	$-\Delta E^M_d$	$\Delta C/CL$
C(20):C(8)PC	34.65	34.87	14.19	13.97	0.826
C(19):C(9)PC	37.38	31.60	9.98	15.76	0.758
C(18):C(10)PC	35.10	29.05	10.48	16.53	0.688
C(17):C(11)PC	36.93	30.36	7.13	13.70	0.603
C(16):C(12)PC	35.70	31.19	6.58	11.09	0.513
C(15):C(13)PC	36.58	33.49	4.18	7.27	0.404
C(14):C(14)PC	35.90	34.38	3.14	4.90	0.283
C(13):C(15)PC	35.49	34.25	2.37	3.61	0.138
C(12):C(16)PC	35.20	35.54	1.90	1.56	0.027
C(11):C(17)PC	35.74	35.01	2.52	3.25	0.189
C(10):C(18)PC	35.31	34.18	3.87	5.00	0.322
C(9):C(19)PC	35.45	32.00	6.03	9.48	0.442
C(8):C(20)PC	34.87	30.96	7.61	11.52	0.541
C(7):C(21)PC	34.89	31.40	9.91	13.40	0.634

* All of the energy terms have the unit of kcal/mol. The term ΔE^P is calculated from the values of E^P_d and E_m as follows: $\Delta E^P_d = E^P_d - 2E_m$. Similarly, $\Delta E^M_d - 2E_m$. The values of E_m are taken from Table 4, column 2. $\Delta C/CL$ is the normalized chain length difference between the *sn*-1 and *sn*-2 acyl chains; only the absolute value of ΔC is used in calcultaing the value of $\Delta C/CL$.

phosphatidylcholines with ΔC values near 0.0 are not as stable as those formed from phosphatidylcholines with larger absolute ΔC values. Furthermore, a partially interdigitated dimer comprising phosphatidylcholine molecules with ΔC of nearly 0.0 is slightly more stable than a mixed interdigitated dimer comprising the same molecular species.

Fig. 5 *c* illustrates the equilibrium structure of a C(18):C(10)PC trans-bilayer dimer packed in the mixed interdigitated motif. This energy-minimized structure illustrates perfectly how the sum of two shorter *sn*-2 acyl chain lengths can be arranged to match equivalently with the overall effective chain length of the longer *sn*-1 acyl chain. Each linear segment of the *sn*-2 acyl chain that extends from C_2 to the terminal C_{10} methyl group is in closest contact with a *sn*-1 acyl chain on each side of its zigzag plane. In addition, the bulky carbonyl oxygens of the *sn*-1 acyl chains are pointing away from the *sn*-2 acyl chain; hence, they are not in a position to affect the chain-chain contact interactions in a mixed interdigitated dimer. In contrast, the bulky carbonyl oxygens of the *sn*-1 acyl groups in a mixed interdigitated C(7):C(21)PC dimer are inserted into a space between two adjacent chains (Fig. 5 *a*), thereby rendering the possibility of perturbing the closest chain-chain contact interactions around them. Of the six examples shown in Figs. 4 and 5, the C(18):C(10)PC trans-bilayer dimer with a mixed interdigitated motif can be expected to have the lowest overall steric energy due to its most extensive inter- and intramolecular chain-chain contact interactions. MM calculations indeed confirm this to be the case; the steric energy is 29.05 kcal/mol, which is 2.35 kcal/mol less than the value calculated for a C(7):C(21)PC trans-bilayer dimer packed in the same mixed interdigitated mode. The intermolecular interaction energy, $\Delta E_d{}^M$, for the equilibrium structure of a C(18):C(10)PC trans-bilayer dimer is calculated to be $(29.05 - 2 \times 22.79) = -16.53$ kcal/mol, which is significantly smaller than the corresponding values calculated for all other energy-minimized trans-bilayer dimers shown in Figs. 4 and 5.

What have we learned from the six examples shown in Figs. 4 and 5? First, when C(X):C(Y)PC are packed in the partially interdigitated motif, only even carbons in the *sn*-1 acyl chains are in closest van der Waals contacts with the adjacent *sn*-2 acyl chain. The magnitudes of the chain-chain contact interactions in a dimeric C(X):C(Y)PC thus depend on whether the values of X and Y are even or odd. MM calculations show that for lipids with similar values of $\Delta C/CL$ the odd-chain lipids have slightly higher values of $E_d{}^P$ than the even-chain lipids (Table 3). Second, the chain-chain contact interactions in mixed interdigitated dimers depends strongly on the absolute ΔC value of the lipid species. For a homologous series of dimeric C(X):C(Y)PC with $X \geq Y$ such as C(14):C(14)PC, C(15):C(13)PC, C(16):C(12)PC, C(17):C(11)PC, C(18):C(10)PC, C(19):C(9)PC and C(20):C(8)PC, the magnitude of the steric energy ($E_d{}^M$) decreases from 34.38 kcal/mol for C(14):C(14)PC (ΔC = 4.67 Å) to 29.05 kcal/mol for C(18):C(10)PC (ΔC = 14.84 Å). In the case of C(18):C(10)PC, the sum of two shorter *sn*-2 acyl chains matches perfectly with the longer *sn*-1 acyl chain, resulting in the maximal chain-chain contact interactions (Fig. 5 *c*). This maximal chain-chain contact is reflected by the smallest value of $E_d{}^M$. Beyond C(18):C(10)PC, the ΔC value is bigger than the sum of two shorter chain lengths; consequently, the chain-chain contact interactions in C(19):C(9)PC and C(20):C(8)PC trans-bilayer dimers are less extensive. Their $E_d{}^M$ values are, therefore, larger (Table 3). For C(X):C(Y)PC with $X < Y$, the steric energy, $E_d{}^M$, also depends heavily on the absolute ΔC value. For the homologous series of C(12):C(16)PC, C(11):C(17)PC, C(10)C(18)PC, C(9):C(19)PC, C(8):C(20)PC, and C(7):C(21)PC, the $E_d{}^M$ value decreases progressively from 35.54 kcal/mol for dimeric C(12):C(16)PC to 30.96 kcal/mol for dimeric C(8):C(20)PC. It is particularly noticeable in the C(8):C(20)PC dimer that the terminal methyl group of the fully extended *sn*-2 acyl chain is spatially in close proximity to C_2 of the adjacent *sn*-1 acyl chain. Consequently, the sum of inter- and intramolecular chain-chain contact interactions are optimal in this C(8):C(20)PC trans-bilayer dimer with a mixed interdigitated packing modif, resulting in the smallest $E_d{}^M$ value. As the absolute ΔC value continues to increase, the

next lipid is C(7):C(21)PC. The *sn*-1 acyl chain of this dimeric lipid extends beyond the bulky carbonyl oxygen (Fig. 5 *a*); consequently, the chain-chain contact interactions are reduced somewhat because of the perturbing effect of carbonyl oxygens. The E_d^M value is thus increased (Table 3). Third, the intermolecular interaction energy reflects primarily the lateral chain-chain interaction which, for mixed-chain phosphatidylcholines, depends on the packing model and the absolute ΔC (or $\Delta C/CL$) value. For highly asymmetric C(*X*):C(*Y*)PC, the trans-bilayer dimer has an overlapping region in which substantial intermolecular chain-chain contact interactions take place; these interactions contribute to the structural stability of the trans-bilayer dimer. Data summarized in Table 3 show that the values of ΔE_d^M and ΔE_d^P decrease with increasing value of $\Delta C/CL$. At a common value of $\Delta C/CL$, ΔE_d^M is, except for C(12):C(16)PC and C(20):C(8)PC, more negative than ΔE_d^P (Table 3). It should be noted that in the mixed interdigitated packing mode, there are three layers of parallel hydrocarbon chains within a trans-bilayer dimer. In the partially interdigitated packing mode, however, there are only two. At a common value of $\Delta C/CL$, the intermolecular chain-chain contact interactions are thus expected to be more extensive in the three-chain system than those in the two-chain system. The intermolecular interactions in the mixed interdigitated packing motif should be expected, therefore, to make a larger negative (stabilizing) contribution to the overall energy. These expectations are indeed borne out by comparing the ΔE_d^M and ΔE_d^P values shown in Table 3.

Packing geometries of tetrameric C(*X*):C(*Y*)PC and their stabilization energies

In the preceding section, we have gained considerable knowledge concerning the structures and energies of C(*X*):C(*Y*)PC trans-bilayer dimers packed optimally in two kinds of motif. These trans-bilayer dimers, however, cannot be regarded as bilayer models, since lateral lipid-lipid interactions within each monolayer of the lipid bilayer are completely lacking in these simple aggregates. In order to mimic the lipid bilayer structure, higher orders of lipid aggregates must be considered. In this section, tetramers of a series of 14 C(*X*):C(*Y*)PC built on their energy-minimized trans-bilayer dimers are constructed. Moreover, the stabilization energies of these tetramers are compared.

When two trans-bilayer dimers of a specific molecular species of C(*X*):C(*Y*)PC aggregate to form a tetramer, there are two simple ways to pair up the two dimers. In one way, two trans-bilayer dimers are staggered when viewed along the *z*-axis. As one trans-bilayer dimer superimposes against the other, then the closest and the strongest interdimeric contacts are between the (*sn*-1)–(*sn*-1) and the (*sn*-2)–(*sn*-2) acyl chains. This type of tetramer is called the front-to-back (F-B) tetramer. Fig. 6 (*a* and *b*) shows the F-B tetramer for the partially interdigitated and the mixed interdigitated dimer of C(18):C(10)PC, respectively. The end-on geometry of each tetramer down the *x*-axis is also presented in Fig. 6 (*a* and *b*). If the two trans-bilayer dimers are aligned side by side and lie on a common plane (the *x*-*y* plane), this type of tetramer is called the up-and-down (U-D) tetramer. Two types of the U-D tetramer for the partially interdigitated and the mixed interdigitated dimers of C(18):C(10)PC generated from the computer graphics are illustrated in Fig. 6 (*c* and *d*, respectively). The graphics displayed view of a projection down the long molecular axis for each tetramer is also included in Fig. 6 (*c* and *d*). Based on the computer graphics it is evident that the largest dimer-dimer contact interaction is the mixed F-B type shown in Fig. 6 *b* with a $E_{F\text{-}B}^M$ value of −8.52 kcal/mol. The weakest dimer-dimer contact interaction, however, is the mixed U-D type (Fig. 6 *d*), with a $E_{U\text{-}D}^M$ value of 46.21 kcal/mol; this is due to the fact that the overall chain length across the trans-bilayer dimer is smaller in the mixed interdigitated packing motif than that in the partially interdigitated packing motif. The stabilization energy of the tetramer contributed by the individual monomer is the normalized difference between the E_s value of the tetramer and the E_s value of the monomer as follows: $\Delta E = (E_{tetramer} - 4\,E_{monomer})/4$. For C(18):C(10)PC, four ΔE values can be calculated based on the monomeric value of E_m, 22.79 kcal/mol, given in Table 2 and the four E_s values for the tetramers shown in Fig. 6. These stabilization energies are: $\Delta E^P_{F\text{-}B} = -21.28$ kcal/mol, $\Delta E^P_{U\text{-}D} = -11.33$ kcal/mol, $\Delta E^M_{F\text{-}B} = -24.92$ kcal/mol, and $\Delta E^M_{U\text{-}D} = -11.24$ kcal/mol, where the superscripts P and M denote the partially interdigitated and mixed interdigitated packing motifs, respectively. The overall averaged stabilization for each of the two motifs of tetramer contributed by the monomer (ΔE^P_{ave} or ΔE^M_{ave}) is the sum of $\Delta E_{F\text{-}B}$ and $\Delta E_{U\text{-}D}$ divided by 2; hence, two overall averaged stabilization energies can be calculated for C(18):C(10)PC. If two tetrameric C(18):C(10)PC are packed according to the partially interdigitated motif in which one tetramer has the F-B arrangement while the other has the U-D arrangement, then the overall averaged stabilization energy, ΔE^P_{ave}, is −16.31 kcal/mol. If the same C(18):C(10)PC molecular species are packed in the mixed interdigitated motif, then the overall averaged stabilization energy, ΔE^M_{ave}, is −18.08 kcal/mol. The relatively smaller value of ΔE^M_{ave} thus suggests that C(18):C(10)PC molecules prefer to self-assemble into the mixed interdigitated motif. The same analysis has been extended to 13 other molecular species of C(*X*):C(*Y*)PC. The results are summarized in Table 4.

Based on data obtained from MM calculations shown in Table 4, it is evident that the strength of steric energy calculated for a C(*X*):C(*Y*)PC tetramer depends on the normalized chain length difference of the two acyl chains in C(*X*):C(*Y*)PC and the geometric arrangement of the nearest neighbors (F-B against U-D) in a defined packing motif. The overall averaged stabilization energy of the two kinds of tetramer (F-B and U-D) contributed by its monomers for each molecular species of C(*X*):C(*Y*)PC can, therefore, have two values due to the presence of two types of packing motif. These values of ΔE^P_{ave} and ΔE^M_{ave} are plotted in Fig. 7 against the normalized chain length difference ($\Delta C/CL$).

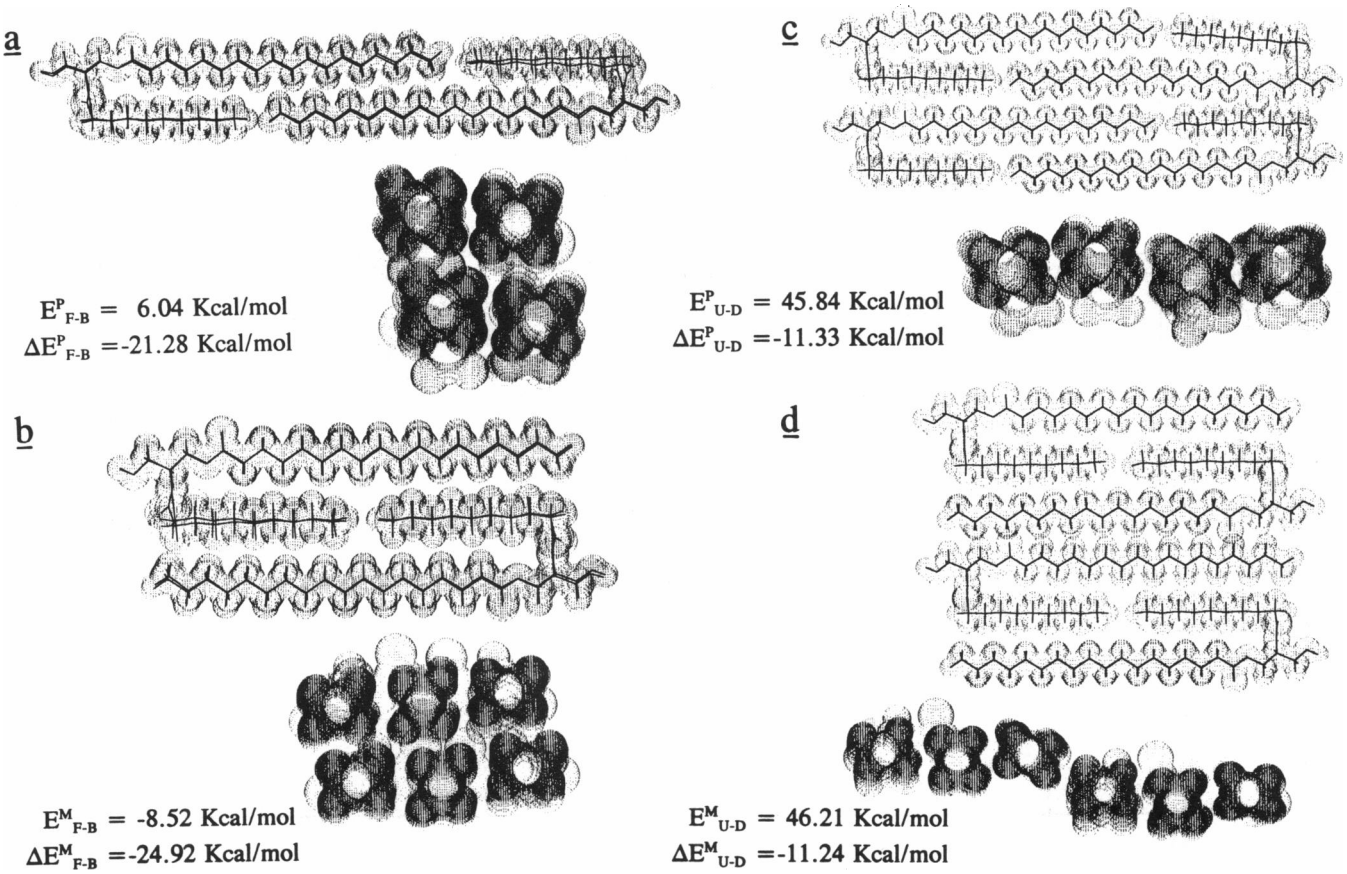

FIGURE 6 The computer-generated figures for energy-minimized tetrameric C(18):C(10)PC with front-to-back (*F-B*) and up-and-down (*U-D*) nearest neighbor arrangements. (*a*) Two pairs of the partially interdigitated dimers are staggered along the *z*-axis to form the F-B tetramer. (*b*) Two pairs of the mixed interdigitated dimers are staggered along the *z*-axis to form the F-B tetramer. (*c*) Two pairs of the partially interdigitated dimers are aligned side by side and lie on a common plane to form the U-D tetramers. (*d*) Two pairs of the mixed interdigitated dimers are arranged in the U-D tetramers. The end-on geometry, along the *x*-axis, of each type of the four tetramers is also presented under the corresponding *x-y* view of each of the four tetramers shown in (*a*)-(*d*).

TABLE 4 The steric energies of tetramers obtained with a series of 14 molecular species of phospholipids*

Lipid	E^{P}_{F-B}	E^{P}_{U-D}	E^{M}_{F-B}	E^{M}_{U-D}	$-\Delta E^{P}_{F-B}$	$-\Delta E^{P}_{U-D}$	$-\Delta E^{P}_{ave}$	$-\Delta E^{M}_{F-B}$	$-\Delta E^{M}_{U-D}$	$-\Delta E^{M}_{ave}$
C(20):C(8)PC	4.45	45.77	5.44	59.16	23.31	12.98	18.15	23.06	9.63	16.35
C(19):C(9)PC	9.49	45.31	-3.31	43.72	21.31	12.35	16.83	24.51	12.75	18.63
C(18):C(10)PC	6.04	45.84	-8.52	46.21	21.28	11.33	16.31	24.92	11.24	18.08
C(17):C(11)PC	10.74	46.10	-5.51	51.85	19.34	10.51	14.93	23.41	9.07	16.24
C(16):C(12)PC	7.27	47.30	-3.04	51.78	19.32	9.32	14.32	21.90	8.20	15.05
C(15):C(13)PC	11.36	48.79	3.36	62.06	17.54	8.18	12.86	19.54	4.87	12.21
C(14):C(14)PC	7.47	47.98	6.68	64.10	17.65	7.53	12.59	17.85	3.50	10.68
C(13):C(15)PC	7.98	46.88	5.35	67.30	16.94	7.21	12.08	17.59	1.96	9.78
C(12):C(16)PC	8.13	47.19	9.33	70.11	16.52	6.75	11.14	16.22	1.02	8.62
C(11):C(17)PC	10.31	48.14	8.00	68.14	16.55	7.10	11.83	17.13	2.10	9.62
C(10):C(18)PC	9.23	48.31	5.51	60.88	17.28	7.51	12.40	18.21	4.37	11.29
C(9):C(19)PC	10.15	46.98	0.48	54.03	18.20	9.00	13.60	20.62	7.23	13.93
C(8):C(20)PC	8.37	46.80	-3.48	46.82	19.15	9.54	14.35	22.11	9.54	15.83
C(7):C(21)PC	9.45	45.16	-2.72	43.46	20.04	11.11	15.58	23.08	11.54	17.31

* All energy terms (E) have the unit of kcal/mol. The various stabilization energy terms have the following expressions: $\Delta E^{P}_{F-B} = (E^{P}_{F-B} - 4E_m)/4$; $\Delta E^{P}_{U-D} = (E^{P}U\text{-}D - 4E_m)/4$; and $\Delta E^{P}ave = (\Delta E^{P}_{F-B} + \Delta E^{P}_{U-D})/2$. Similar expressions are used for ΔE^{M}_{F-B}, ΔE^{M}_{U-D}, and ΔE^{M}_{ave}.

Clearly, C(X):C(Y)PC with $\Delta C/CL$ values equal to or smaller than 0.41 have larger negative values of ΔE^{P}_{ave}, indicating that these C(X):C(Y)PC can make a larger negative (stabilizing) contribution to the averaged tetramer structure with partially interdigitated packing motif. However, highly asymmetric C(X):C(Y)PC with $\Delta C/CL$ values greater than 0.41 but smaller than 0.80 have larger negative values of ΔE^{M}_{ave}. These highly asymmetric phosphatidylcholines thus make larger stabilizing contributions to the average structure of tetramers characterized by mixed interdigitated packing motif. It should be emphasized that the nearest neighbors of our tetramer model have two kinds of geometric arrange-

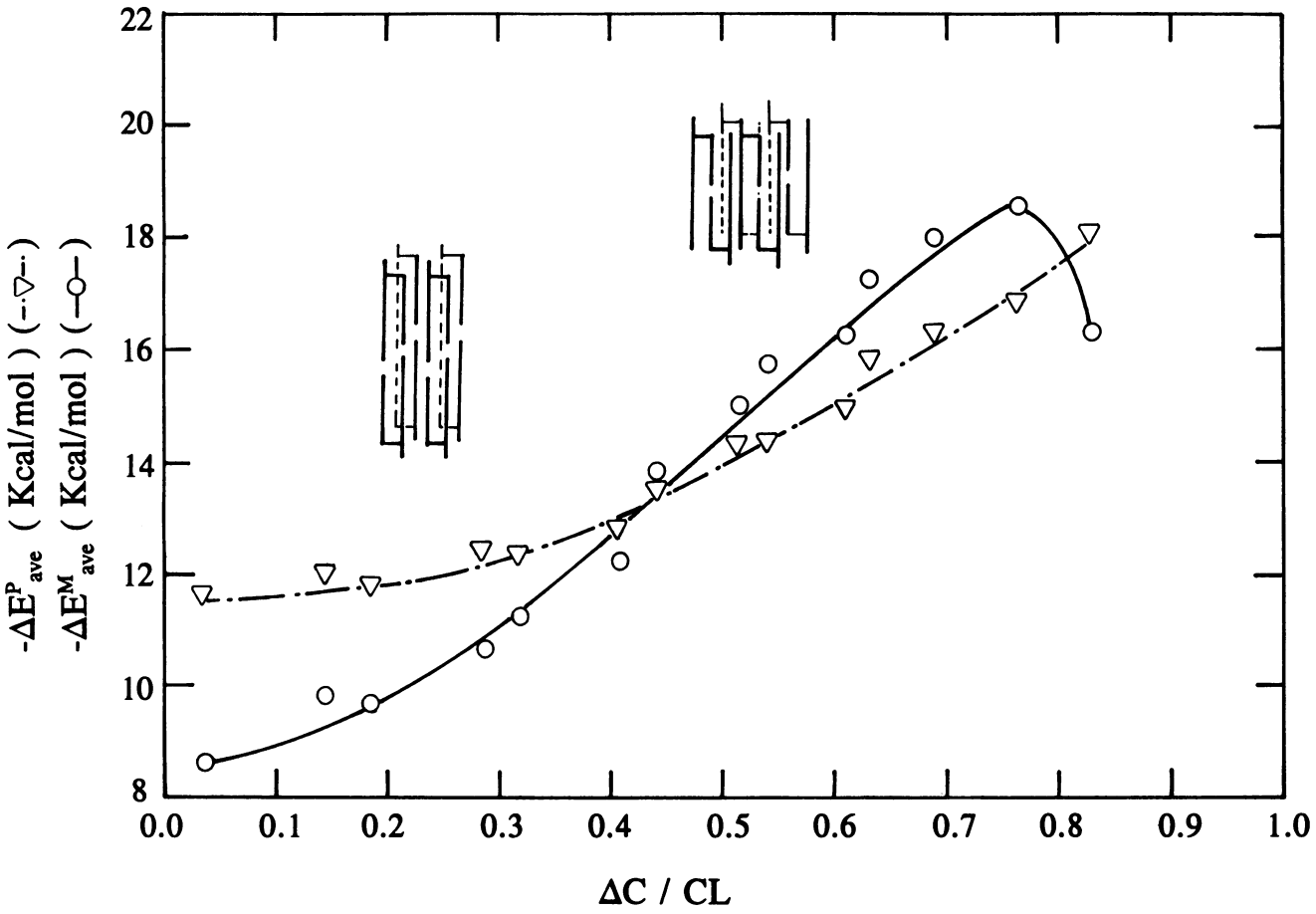

FIGURE 7 The overall averaged stabilization energy of tetrameric C(X):C(Y)PC versus the structural parameter $\Delta C/CL$ of C(X):C(Y)PC. The values of ΔE^{P}_{ave} and ΔE^{M}_{ave} are taken from Table 4, and the values of $\Delta C/CL$ are taken from Table 3. Lipids with larger negative values of ΔE^{P}_{ave} are shown schematically to assemble into the partially interdigitated packing motif, and those with larger negative values of ΔE^{M}_{ave} are shown schematically to assemble into the mixed interdigitated packing motif.

ment, F-B and U-D. The averaged sum of these two kinds of geometric arrangement is taken to mimic, to a first approximation, the orthorhombic closed-packed structure of phospholipids in the plane of the lipid bilayer. The results shown in Fig. 7 perhaps can be reasonably used to interpret the properties of the lipid bilayer. Consequently, we can conclude that C(X):C(Y)PC with $\Delta C/CL$ values equal to or smaller than 0.41 are preferably assembled into the partially interdigitated bilayer. In contrast, highly asymmetric C(X):C(Y)PC with a $\Delta C/CL$ value greater than 0.41 prefer to self-assemble into the mixed interdigitated bilayer. These conclusions are in complete accord with the experimental results obtained calorimetrically for a series of C(X):C(Y)PC with a common MW of 678.0 (Lin et al., 1991). Specifically, the T_m (or ΔH) values of this series of phospholipids obtained from DSC experiments exhibit a biphasic profile in the T_m (or ΔH) versus $\Delta C/CL$ plot. Below the $\Delta C/CL$ value of 0.41, the T_m (or ΔH) value decreases nearly linearly with increasing $\Delta C/CL$. Beyond the minimum $\Delta C/CL$ value of 0.41, the T_m value of the highly asymmetric phosphatidylcholines increases with increasing $\Delta C/CL$. This biphasic phenomenon has been interpreted to reflect that phospholipids with $\Delta C/CL$ less than 0.41 are packed in the partially interdigitated bilayer and highly asymmetric phospholipids with $\Delta C/CL$ greater than 0.41 are packed in the mixed interdigitated bilayer at $T < T_m$ (Huang, 1990; Lin et al., 1991). The computational results obtained from MM calculations shown in Fig. 7 thus provide strong support for our earlier interpretation of the biphasic phenomena observed for four series of C(X):C(Y)-PC. Moreover, the transition of C(X):C(Y)PC from a partially interdigitated to a mixed interdigitated packing motif is observed in Fig. 7 to take place at $\Delta C/CL$ slightly above 0.41; this again is in complete accord with the calorimetric results detected for the same series of C(X):C(Y)PC (Lin et al., 1991). In summary, the computational results presented in this paper and the experimental results presented previously are consistent, and the biphasic effect of lipid chain asymmetry on the phase transition behavior is thus firmly established and can now be considered as a general property of the lipid bilayer.

CONCLUSIONS

Phosphatidylcholines, quantitatively the most abundant lipids in animal cell membranes, consist of a large number of molecular species characterized by the same headgroup but

widely different acyl chains. Although some of the structure-property relationships of identical-chain phosphatidylcholines or C(*X*):C(*X*)PC in the lipid bilayer are known, quantitative information regarding the vast structure-property relationships of mixed-chain phosphatidylcholines or C(*X*):C(*Y*)PC has remained, to a large degree, elusive. Recently, work in this laboratory has been directed toward obtaining quantitative information regarding the structure-property relationships of mixed-chain phospholipids (Huang, 1993a,b), and the work described in this communication is an extension of our continuous efforts in this regard.

MM calculations have been carried out in this study to determine the energy-minimized structures and steric energies for a homologous series of 14 mixed-chain phosphatidylcholines with MW identical to that of C(14):C(14)PC. In addition, dimers and tetramers of these 14 molecular species assembled in the partially interdigitated and mixed interdigitated packing motifs are also examined. Based on the results of our extensive MM calculations, the following conclusions can be drawn:

1. The energy-minimized structure of C(14):C(14)PC in the crystalline state is characterized by two nearly parallel acyl chains (Fig. 2). The zigzag planes of these two acyl chains, however, are virtually perpendicular to each other (Figs. 2 and 3). This packing geometry is qualitatively similar to the crystal structure B of the same lipid species determined by x-ray diffraction (Pearson and Pascher, 1979; Pascher et al., 1992). Moreover, the steric energy of the energy-minimized structure is considerably smaller than that of crystal structures A and B.

2. The overall strength of intermolecular chain-chain contact interactions in a C(*X*):C(*Y*)PC trans-bilayer dimer depends on the lipid chain asymmetry (ΔC) and the type of chain packing motif (the partially interdigitated versus the mixed interdigitated). In general, C(*X*):C(*Y*)PC with larger ΔC values usually have larger negative values of intermolecular interaction energy (ΔE_d). Also, asymmetric lipids packed in the mixed interdigitated motif have smaller values of steric energy.

3. When two dimeric C(*X*):C(*Y*)PC are aggregated to form tetramers, the nearest neighbors can orient into two different types of geometric arrangement. One trans-bilayer dimer can superimpose against the other to form a front-to-back tetramer, or one trans-bilayer dimer can align side-by-side with the other to form an up-and-down tetramer. When these two types of geometry are considered jointly, these multiple tetramers can be viewed, to a first approximation, as a simple model for the lipid bilayer. Since the trans-bilayer dimer can have the partially interdigitated or the mixed interdigitated packing motif, two models of the lipid bilayer (the partially interdigitated and the mixed interdigitated models) can thus be mimicked by multiple tetramers. Results of MM calculations indicate that C(*X*):C(*Y*)PC with $\Delta C/CL$ smaller than 0.41 are preferably assembled into the partially interdigitated bilayer and C(*X*):C(*Y*)PC with $\Delta C/CL$ greater than 0.41 prefer to assemble into the mixed interdigitated bilayer (Fig. 7). These computational results are in complete accord with the experimental data obtained calorimetrically from this laboratory (Lin et al., 1991).

The secretarial assistance of Ms. Linda Saunders is gratefully acknowledged.

This research was supported, in part, by U.S. Public Health Service Grant GM-17452 from the National Institute of General Medical Sciences, National Institutes of Health, Department of Health and Human Services.

REFERENCES

Allinger, N. L. 1977. Conformational analysis. 130. MM2. A hydrocarbon force field utilizing V_1 and V_2 torsional terms. *J. Am. Chem. Soc.* 99: 8127–8134.

Bultmann, T., H-n. Lin, Z-q. Wang, and C. Huang. 1991. Thermotropic and mixing behavior of mixed-chain phosphatidylcholines with molecular weights identical with that of L-α-dipalmitoylphosphatidylcholine. *Biochemistry.* 30:7194–7202.

Huang, C. 1977. A structural model for the cholesterol-phosphatidylcholine complexes in bilayer membranes. *Lipids.* 12:348–356.

Huang, C. 1990. Mixed-chain phospholipids and interdigitated bilayer systems. *Klin. Wochenschr.* 68:149–165.

Huang, C., Z-q. Wang, H-n. Lin, and E. E. Brumbaugh. 1993a. Calorimetric studies of fully hydrated phosphotidylcholines with highly asymmetric acyl chains. *Biochim. Biophys. Acta.* 1145:298–310.

Huang, C., S. Li, Z-q. Wang, and H-n. Lin. 1993b. Dependence of the bilayer phase transition temperatures on the structural parameters of phosphatidylcholines. *Lipids.* 28:365–370.

Hui, S. W., J. T. Mason, and C. Huang. 1984. Acyl chain interdigitation in saturated mixed-chain phosphatidylcholine bilayer dispersions. *Biochemistry.* 23:5570–5577.

Lewis, R. N. A. H., and R. N. McElhaney. 1992. Structures of the subgel phases of *n*-saturated diacyl phosphatidylcholine bilayer: FTIR spectroscopic studies of $^{13}C{=}O$ and ^{2}H labelled lipids. *Biophys. J.* 61:63–77.

Lin, H-n., Z-q. Wang, and C. Huang. 1990. Differential scanning calorimetry study of mixed-chain phosphatidylcholines with a common molecular weight identical with diheptadecanoylphosphatidylcholine. *Biochemistry.* 29:7063–7072.

Lin, H-n., Z-q. Wang, and C. Huang. 1991. The influence of acyl chain-length asymmetry on the phase transition parameters of phosphatidylcholine dispersions. *Biochim. Biophys. Acta.* 1067:17–28.

Mason, J. T., C. Huang, and R. L. Biltonen. 1981. Calorimetric investigations of saturated mixed-chain phosphatidylcholine bilayer dispersions. *Biochemistry.* 20:6086–6092.

Mattai, J., P. K. Sripada, and G. G. Shipley. 1987. Mixed-chain phosphatidylcholine bilayers: structure and properties. *Biochemistry.* 26:3287–3297.

McIntosh, T. J., S. A. Simon, J. C. Ellington, Jr., and N. A. Porter. 1984. New structural model for mixed-chain phosphatidylcholine bilayers. *Biochemistry.* 23:4038–4044.

Nambi, P., E. S. Rowe, and T. J. McIntosh. 1988. Studies of ethanol-induced interdigitated gel phase in phosphatidylcholines using the fluorophore 1,6-diphenyl-1,3,5-hexatriene. *Biochemistry.* 27:9175–9182.

Ohki, K., K. Tamura, and I. Hatta. 1990. Ethanol induces interdigitated gel phase ($L_{\beta I}$) and ripple phase ($P_{\beta'}$) in phosphatidylcholine membranes: a scanning density meter study. *Biochim. Biophys. Acta.* 1028:215–222.

Pascher, I., M. Lundmark, P-G. Nyholm, and S. Sundell. 1992. Crystal structures of membrane lipids. *Biochim. Biophys. Acta.* 1113:339–373.

Pearson, R. H., and I. Pascher. 1979. The molecular structure of lecithin dihydrate. *Nature (Lond.).* 281:499–501.

Roth, L. G., and C-H. Chen. 1991. Thermodynamic elucidation of ethanol-induced interdigitation of hydrocarbon chains in phosphatidylcholine bilayer vesicles. *J. Phys. Chem.* 95:7955–7959.

Rowe, E. S. 1983. Lipid chain length and temperature dependence of alcohol lipid interaction. *Biochemistry.* 22:2299–3305.

Rowe, E. S. 1992. Effects of ethanol on membrane lipids. *In* Alcohol and Neurobiology: Receptors, Membranes, and Channels. R. R. Watson, editor. CRC Press, Boca Raton, FL. 239–267.

Ruocco, M. J., and G. G. Shipley. 1982. Characterization of the sub-transition of hydrated dipalmitoylphosphatidylcholine bilayers: x-ray diffraction study. *Biochim. Biophys. Acta.* 684:59–66.

Shah, J., P. K. Sripada, and G. G. Shipley. 1990. Structure and properties of mixed-chain phosphatidylcholine bilayers. *Biochemistry.* 29: 4254–4262.

Sisk R. B., Z-q. Wang, H-n. Lin, and C. Huang. 1990. Mixing behavior of identical molecular weight phosphatidylcholines with various chain-length differences in two-component lamellae. *Biophys. J.* 58:777–783.

Slater, J. L., C. Huang, and I. W. Levin. 1992. Interdigitated bilayer packing motifs: Raman spectroscopic studies on the eutectic phase behavior of the 1-stearoyl-2-caprylphosphatidylcholine/dimyristoylphosphatidylcholine binary mixture. *Biochim. Biophys. Acta.* 1106:242–250.

Vanderkooi, G. 1991. Multibilayer structure of dimyristoylphosphatidylcholine dihydrate as determined by energy minimization. *Biochemistry.* 30:10760–10768.

Wang, Z-q., H-n. Lin, and C. Huang. 1990. Differential scanning calorimetric study of a homologous series of fully hydrated saturated mixed-chain C(X):C(X+6) phosphatidylcholines. *Biochemistry.* 29:7072–7076.

Zhu, T., and M. Caffrey. 1993. Thermodynamic, thermomechanical and structural properties of a hydrated asymmetric phosphatidylcholine. *Biophys. J.* 65:939–954.